Appl. Phys. A (2016) 122:140
DOI 10.1007/s00339-016-9679-5

Applied Physics A
Materials Science & Processing

Monte Carlo simulation of transport coefficient in organic solar cells

S. Khodakarimi[1,2] · M. H. Hekmatshoar[1] · F. Abbasi[2,3]

Received: 24 August 2015 / Accepted: 28 January 2016 / Published online: 11 February 2016

Abstract The Monte Carlo simulation was used to study the charge transport mechanism inside a three-dimensional bulk heterojunction (BHJ) polymer solar cell having an additional layer on the BHJ active layer. In the BHJ section, the P3HT:PCBM ratio was varied and its optimum value, in which the diffusion coefficient reached its maximum value, was determined. The diffusion coefficient and short-circuit current (J_{sc}) were simulated. In low diffusion coefficients, recombination losses limited the performance, which led to a reduction in the short-circuit current. The results showed that adding a P3HT layer having a thickness of 10 nm over the BHJ layer increased hole mobility and enhanced short-circuit current and performance of the solar cells. On the other hand, adding a PCBM layer between the active layer and the cathode side behaved as an efficient hole blocking layer so that electrons could be selectively extracted.

✉ M. H. Hekmatshoar
hekmatshoar@sut.ac.ir

✉ F. Abbasi
f.abbasi@sut.ac.ir

[1] Faculty of Sciences, Sahand University of Technology, Tabriz, Iran

[2] Institute of Polymeric Materials, Sahand University of Technology, Tabriz, Iran

[3] Faculty of Polymer Engineering, Sahand University of Technology, Tabriz, Iran

1 Introduction

Conjugated semiconducting polymers have attracted increasing attention because of their potential applications in electroluminescent devices, field-effect transistors, and solar cells. Operation of these devices highly depends on the characteristics of carrier transport; hence, determination of carrier transport in conjugated polymers has been the subject of numerous investigations [1–3]. The performance of these devices is limited by various factors. For example, a high-energy band gap of the used donor materials limits the capability to harvest the low-energy photons from the sunlight. For this reason, the charge carrier mobility of the organic materials is very low [4].

In the past years, the efficiency of the solar cells based on bulk heterojunctions (BHJs) of organic semiconductors has significantly increased. Solar cells based on regioregular poly(3-hexylthiophene) (P3HT) blended with [6, 6]-phenyl C_{61}-butyric acid methyl ester (PCBM) often have a suitable power conversion efficiency. Research efforts have developed higher efficiency solar cells using various strategies, such as morphology engineering (e.g., via thermal/solvent annealing), interface engineering (e.g., applying anode/cathode interfacial layers), and new donor/acceptor materials development with different frontier energy levels, thereby increasing the energetic distance between the highest occupied molecular orbital (HOMO) of the donor and the lowest unoccupied molecular orbital (LUMO) of the acceptor results in increasing the V_{oc} [5–7].

It is well recognized that the electronic properties of the individual materials as well the morphology of the phase-separated P3HT:PCBM blend play a significant role in the device performance [8]. While a large amount of work has been done on designing molecular structures to optimize their optoelectronic properties, such as HOMO and LUMO

levels and wavelength range over which light is absorbed to enhance the power conversion efficiency (PCE), studies of the morphology–performance relationship are becoming more common and a prerequisite for rationally improving performance [9]. Several approaches have been employed to improve the morphological stability of P3HT/PCBM blends. For example, the film morphology was stabilized using a graft copolymer of P3HT and PCBM [10]. The effects of blend layer morphology changes can be clearly observed in the absorption spectra. Morphologies favorable for good photovoltaic performance typically exhibit more intense absorption with more pronounced peaks [11].

The performance of a BHJ solar cell depends on the mobility as well as the energy levels of the donors and acceptors. The short-circuit current density is mostly determined by the acceptor band gap, whereas the open-circuit voltage is determined by the difference between the HOMO level of the donor and the LUMO level of the acceptor [12].

In organic solar cells, the mobility simultaneously controls both the carrier extraction and the losses via carrier recombination. Recombination is known to be the dominant factor to limit the efficiency through the effect of mobility and increasing the low mobility limit because of the photocarrier accumulation inside the bulk. It is thought that the improvement of the efficiency requires a high mobility because of an easier photocarrier extraction [12]. Mobility is a device parameter rather than a material parameter and is sensitive to the nanoscale morphology of the organic semiconductor thin film. In a van der Waals crystal, the final nanomorphology depends on film preparation. Parameters such as solvent type, the solvent evaporation (crystallization) time, the temperature of the substrate, and/or the deposition method can change the nanomorphology. The formation of a bulk heterojunction enhances the interfacial area between donor and acceptor phases; however, the complicated nanomorphology of a blend is difficult to optimize and control [13].

Bisquert [14] studied chemical diffusion coefficient of dye-sensitized solar cells for a wide but stationary distribution of sites energies, giving the Fermi-level dependent D_n, and for the enhancement of the diffusivity by effect of electrostatic shift of energy levels, which correspond to the mean-field approximation to interaction in a lattice gas. He et al. [15] determined the electron diffusion coefficient in dye-sensitized solar cells at potentials beyond the open-circuit potential. At these potentials, the Warburg feature associated with electron diffusion was observable from the impedance spectra. They showed that D_n remained nearly constant within this potential range. Sanchis et al. [16] determined diffusion–recombination in polymer:fullerene solar cells. The comparison between active layer thickness and the carrier diffusion length allows exclusion of bulk transport losses as a highly detrimental factor for this class of solar cells. Mohan et al. [17] simulated carrier diffusion in organic thin films with morphological inhomogeneity by Monte Carlo simulation. For the homogeneous films, the carrier diffusion was found to decrease upon decreasing the energetic disorder. On the contrary, in the case of inhomogeneous films the carrier diffusion enhanced upon decreasing the overall energetic disorder, up to an optimum value, beyond which the carrier diffusion decreased.

In the present work, Monte Carlo simulation was performed to investigate the charge transport mechanism inside a BHJ active layer. The influences of morphology, ratio of donor and acceptor, and adding a donor layer on diffusion and short-circuit current (J_{sc}) were studied.

2 Simulation

2.1 System morphology

Several theoretical works [14–16] have been done to study the charge mobility in the organic molecular systems. Non-crystalline organic solids, molecularly doped crystals, molecular glasses, and conjugated polymers are characterized by small mean free paths for the charge carriers as a result of high degree of disorder present in the system. Therefore, the elementary transport step is the charge transfer between adjacent transporting elements, which can be either molecules participating in transport or segments of a polymer separated by topological defects. These charge-transporting elements are identified as sites whose energy distributions obey a Gaussian distribution [14]

$$g(\varepsilon) = \frac{1}{\sqrt{2\pi}\sigma}\exp\left(-\frac{\varepsilon^2}{2\sigma^2}\right) \quad (1)$$

where the energy ε is measured relative to the center of the density of states. Within this distribution, all states are localized. The choice of such a distribution was based on the Gaussian profile of the excitonic absorption band as well as on the recognition that the polarization energy is determined by a large number of internal coordinates, which vary randomly a little so the central limit theorem of statistics holds.

A common simplification was to assume a uniform generation rate throughout the active layer. However, experiments and theoretical studies have shown that interference effects can significantly enhance light absorption in certain regions of the film [15]. In the simulated system, each particle (electron, hole, and exciton) is associated with an event of a specific waiting time, τ_q, which is associated with a change in the system. All of the possible events in the system are stored in the order of ascending waiting time. At each time step, the event at the

start of the queue is executed and removed from the queue. All of the waiting times are then reduced by the time expired and newly enabled events are inserted in the queue. In general, a waiting τ_q [18]

$$\tau_q = -\frac{1}{W}\ln(X) \tag{2}$$

can be associated with any event with rate W. X is a random number which is uniformly distributed between 0 and 1. In this simulation, excitons are created at randomly chosen polymer sites at a constant rate. In organic semiconductors, the exciton lifetime is about 500 ps, and the diffusion length of exciton is around 10–20 nm [19].

In this model, the jump rate between two transporting sites i and j is assumed to be of the Miller–Abrahams type:

$$v_{ij} = v_0 e^{\left(-2\gamma R_{ij}\right)} \begin{cases} e^{\left(\frac{-(\varepsilon_j-\varepsilon_i)}{k_B T}\right)} & \varepsilon_j > \varepsilon_i \\ 1, & \varepsilon_j < \varepsilon_i \end{cases} \tag{3}$$

where γ is the wave function decay rate and R_{ij} is the inter-site distance ($2\gamma R_{ij}$ is the wave function overlap parameter governing the electronic exchange interaction between sites). ε_i and ε_j are the effective energies of the sites i and j, which include the electrostatic energy, k_B is the Boltzmann constant, and T is the temperature in Kelvin [16, 17].

The Columbic interaction between sites i and j is calculated as

$$V_{ij} = -\frac{q_i q_j}{4\pi\varepsilon_0\varepsilon}\frac{1}{R_{ij}} \tag{4}$$

where q_i and q_j are the site charges, respectively, ε is the dielectric constant, ε_0 is the vacuum permittivity, and R_{ij} is the distance between sites i and j. The Coulomb interactions between neighboring charges are considered for the charge carriers within a distance less than R_c, cutoff radius [19].

On the other hand, the distance traversed by the charge carriers is given by [20]:

$$l = \mu.\tau.E \tag{5}$$

where μ is the mobility of the charge carriers, τ is their lifetime, and E is the electric field in the device. Thus, the mobility plays a major role in the collection of charge carriers. Charge transport in polymers and organic materials, in general, takes place by hopping among the localized states, which is the bottleneck of the performance of polymer-based solar cells. Fullerenes are blended with polymers to enhance the dissociation of excited state into free carriers and transport free electrons to the electrode. The interaction within the polymer–fullerene complex, therefore, plays a major role in the generation and transport of both electrons and holes [21].

MC simulation was performed to explore the influence of morphology on diffusion and short-circuit current. A bulk heterojunction lattice of 60 × 60 × z (varied), along x, y and z directions, with lattice constant $a = 1$ nm was used for computation which was sandwiched between two layers [22]. The z direction was considered as the direction of the applied bias of working direction. Periodic boundary conditions were applied in both the x and y directions. Hopping was restricted to the adjacent sites. Thus, the particles could be hopped to six adjacent sites in a cubic lattice. The site energies of lattice were initially taken randomly from a Gaussian distribution with mean value $\approx$ 5.1 eV and standard deviation $\sigma = 75$ meV. The homogenous distributions were attributed to the as-cast blended BHJ prior to thermal annealing. For all of homogenous blend ratios, the grid elements' values were populated according to a Gaussian distribution, with the mean value equal to the desired weight ratio and a standard deviation of 0.05. This Gaussian initialization produced a solution close to an ideal mixture, but with entropic effects [23].

Since the charge transport is due to hopping between localized states, the charge carrier mobility depends on electric field and carrier concentration. In disordered systems, the density of states is usually given by an exponential or Gaussian distribution [24]. The center of the steady state distribution is called disorder parameter σ. The center of the steady state charge distribution (density of occupied states distribution) is shifted by σ^2/kT down as compared to the center of the density of states. Photogenerated (and injected) charge carriers can be generated at higher energies, followed by a relaxation of the charge carriers to a quasi-equilibrium.

Another important factor which can negatively influence the solar cell performance is electronic trap states, since they lower the mobility, disturb the internal field distribution, and can act as recombination centers and a decreased mobility may result in a loss of the fill factor [25].

It should be mentioned that the relationship between the scale of electron and hole conductor phase separation is due to device efficiency. Therefore, it must be generated morphologies with varying scales of phase separation. Therefore, a simple method was chosen to generate morphologies being qualitatively reasonable. For the cubic lattice of hopping sites, the sites were initially assigned randomly as either hole or electron conductors with equal probability. The Ising Hamiltonian for the energy of site i is [18]

$$\epsilon_i = -\frac{J}{2}\sum_j \left(\delta_{S_i S_j} - 1\right) \tag{6}$$

where $\delta_{S_i S_j}$ is the delta function and s_i and s_j are the spins occupying sites i and j. The summation over j includes all first- and second-nearest neighbors, and the energetic

interaction is inversely proportional to the distance between neighboring sites i and j. To obtain a series of morphologies with different phase interpenetrations, an appropriate initial configuration and the corresponding interaction energy, J, were chosen. In this simulation, the initial morphology with minimal phase separation was chosen, and the interaction energy, J, was set as $+1.0\ k_BT$. To relax the system to an energetically favorable state, the neighboring pairs of sites were chosen randomly in the system, and then the acceptance probability for an attempt to swap the site spins was calculated as [19, 26]

$$P(\Delta\varepsilon) = \frac{\exp(-\Delta\varepsilon/(k_BT))}{1+\exp(-\Delta\varepsilon/(k_BT))}. \quad (7)$$

where $\Delta\varepsilon$ is the energy change in the system caused by swapping the site spins. After a large number of attempted spin swappings, a desired morphology series with varying scales of phase separation can be generated and stored for later use [25].

2.2 Diffusion coefficient and mobility

Macroscopically, for an electric field with an intensity of E and a carrier density gradient $\frac{dn}{dx}\left(\frac{dp}{dx}\right)$, the carrier current density can be written as [24, 27]:

$$J_n = -\mu_n nE - D_n\frac{dn}{dx}$$
$$J_p = -\mu_p pE - D_p\frac{dp}{dx} \quad (8)$$

where $\mu_n(\mu_p)$ and $D_n(D_p)$ are positive constants called mobility and diffusion coefficient, respectively, and x is an arbitrary space coordinate. The mobility describes the response of a charge carrier to an applied electric field. It is defined as the magnitude of the velocity of the charge carriers, usually called the drift velocity, v_d, which is divided by the magnitude of the electric field. This definition is valid for both electrons and holes and makes the mobility to get a positive quantity.

$$\mu_n = \frac{v_d(e)}{E}, \quad \mu_p = \frac{v_d(p)}{E} \quad (9)$$

where μ_n and μ_p are mobility of electron and hole, respectively. In the thermal equilibrium, diffusion coefficient is related to mobility by the Einstein relation [24, 28, 29]

$$\mu_n = \frac{eD_n}{k_BT}, \quad \mu_p = \frac{eD_p}{k_BT}. \quad (10)$$

Although the disordered in considered organic semiconductors exhibits charge carrier mobilities which are several orders of magnitude lower than those for inorganic crystals, the resulting solar cells show adequate mobilities. As discussed, the mobility has direct influence on several processes including polaron pair dissociation, charge transport, and charge extraction, which are important for efficient organic solar cells.

Fig. 1 Plots showing the example morphologies generated by minimization of an Ising Hamiltonian. Electron and hole conductors are displayed as white and dark shades, respectively. **a** An unrelaxed morphology and **b** the morphology after 10^6 MC steps (P3HT:PCBM = 1:1). Density of states (DOS) of disordered P3HT (**c**) and PCBM (**d**) domains

The band bending, responsible for a major part of the difference between polaron pair energy and open-circuit voltage, depends on the charge carrier mobility [12].

In the MC simulation, the position of the carrier as a function of time is monitored and the temporal evolution of diffusion coefficient is calculated by the equation [17, 30, 31]

$$D_z = \frac{(Z-Z)^2}{2t} \quad (11)$$

The diffusion coefficient was calculated along the applied bias of working direction (D_z calculated along z direction) at $T = 300$ K. It describes the average mean square displacement of a carrier with time.

In homogeneous films, stronger disorder leads to smaller values for the mobility, which is due to the barriers that a carrier has to overcome. It is somewhat difficult to separate these still strongly Coulomb bound charge carrier pairs due to the increased disorder. Also, it is more likely that the trapped charge carriers recombine with mobile ones. However, the positive effects on the device performance outweigh the drawbacks. For an efficient BHJ solar cell, a good control of the morphology is very important [24].

The most important factor in a solar cell is the power conversion efficiency, η. It is based on the parameters open-circuit voltage V_{oc} (two different energy levels which can govern the open-circuit voltage: first, the effective band gap corresponding to the energy of the polaron pair after exciton dissociation, thus depending on donor and acceptor energetics, and second, the difference between the work functions of anode and cathode [25]), short-circuit current density J_{sc}, and fill factor FF [12]. The fill factor is given by the quotient of maximum power, the product of open-circuit voltage and short-circuit current. The efficiency is the ratio of maximum power to incident radiant power P_L typically radiated by the sun

$$\eta = \frac{FFj_{sc}V_{oc}}{P_L}. \quad (12)$$

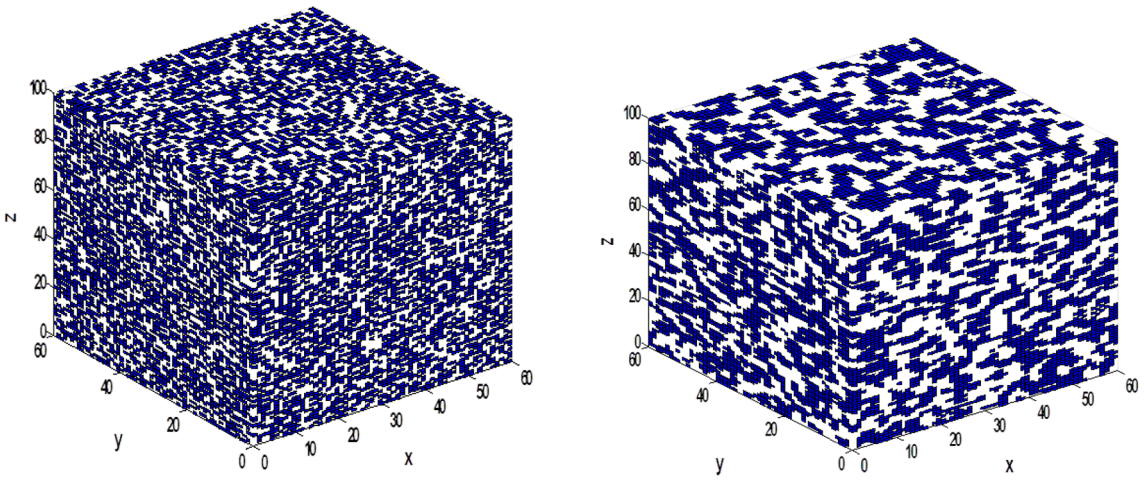
z
y
x
0
20
40
60
80
100
10
30
50

(a) (b)

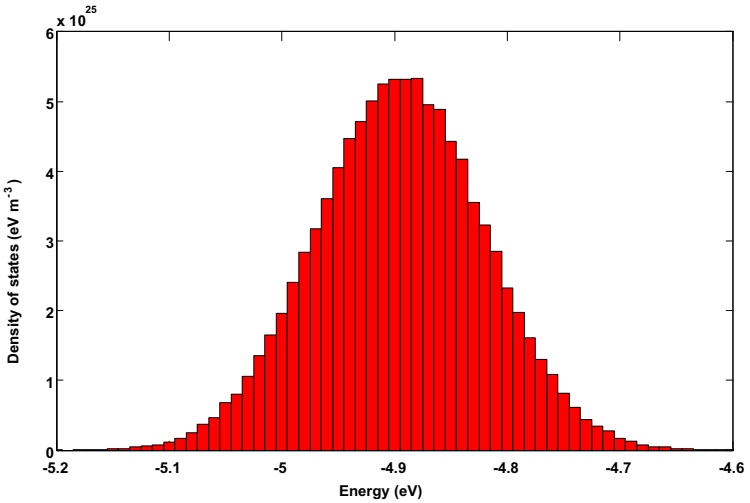
x 10^25
Density of states (eV m^-3)
Energy (eV)
0
1
2
3
4
5
6
-5.2
-5.1
-5
-4.9
-4.8
-4.7
-4.6

(c)

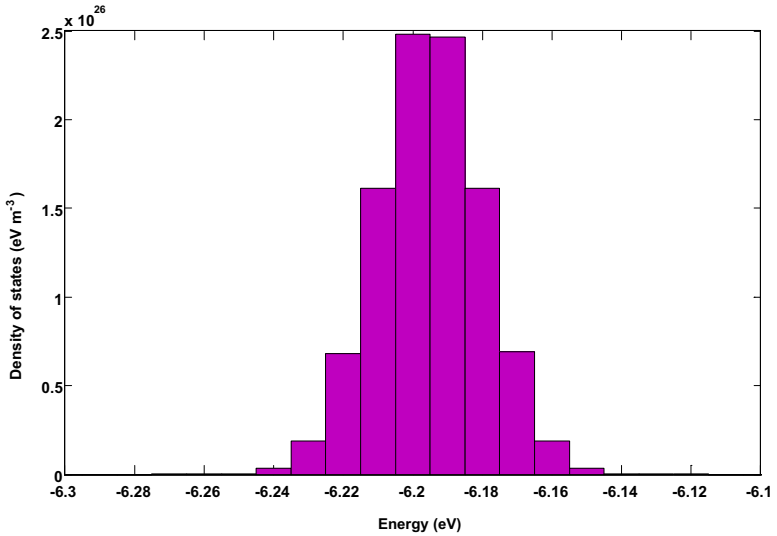
x 10^26
Density of states (eV m^-3)
Energy (eV)
0
0.5
1
1.5
2
2.5
-6.3
-6.28
-6.26
-6.24
-6.22
-6.2
-6.18
-6.16
-6.14
-6.12
-6.1

(d)

3 Results and discussion

To simulate the exciton dissociation dynamics of a BHJ film, a model BHJ morphology was created using the modified Ising model [18] (Fig. 1). To relax the system and to lower the energy state, after a large number of attempted spin swappings, a desired morphology series with varying scales of phase separation can be generated. As simulation proceeds, after lowering energy of the system, the interfacial area between electron and hole conducting phases tends to decrease. Figure 2 shows the interfacial area changes for different thickness of BHJ layer during relaxing the system. In the case of four thicknesses, the interfacial area decreases after relaxing. It also shows that the rate of decrease in interfacial area increases by increase in the thickness of BHJ layer. Figure 1c, d shows density of states (DOS) of donor and acceptor. The site energies of lattice were taken randomly from a Gaussian distribution, which gives the energetic disorder parameter $\hat{\sigma} = \sigma/kT$. It should be mentioned that the standard deviation and mean energy of DOS also influence the charge transport [32, 33].

In the optimal interfacial area between the donor and the acceptor, exciton separation and collection of carriers are balanced. In lower interfacial area, however, the number of exciton produced decreases and the exciton traverses long distance to the interface between the donor and acceptor. Therefore, the small areas of the donor (acceptor) are joined and form larger areas. Under these conditions, the probability of electron–hole recombination reduces and carriers collected by the electrodes increase (Fig. 3).

To determine the optimal interfacial area between donor and acceptor, a series of morphologies were created. The optimal interfacial area is 2×10^6 nm^2 (10^6 MC steps). The donor–acceptor interfacial area determines the probability that electron and hole meet the interfacial area available for electron–hole encounter and recombination, which plays an essential role in solar cells. The enhanced interface leads to significantly increased electron–hole recombination losses both around the short-circuit current and maximum power point, which is determined in complement with J–V characterization. There is therefore an opportunity to increase open-circuit voltage (V_{oc}) beyond current limits by reducing the donor–acceptor interfacial area. To simulate exciton behavior in the P3HT phase, a list of simulation parameters were taken from Table 1 [18].

Figure 4 shows jump diffusion coefficient (D_J), which describes the average mean square displacement of a carrier with time as a function of thickness of BHJ layer. Here, diffusion with waiting time can be represented by a particle jumping to its neighboring sites and remaining stationary for some time before attempting another jump. The charge is then forced to remain at that site for time t. At that time, the particle jumps to one of its nearest lattice sites [35]. It is shown that D_J increases with increasing thickness for both relaxed and unrelaxed systems. D_J, derived from unrelaxed layer, starts to increase slightly. In particular, relaxing leads to diffusion of PCBM from blended regions to PCBM-rich regions. The resultant morphology consists of two distinct regions and helps to merge smaller domains into the larger interconnected ones and, consequently,

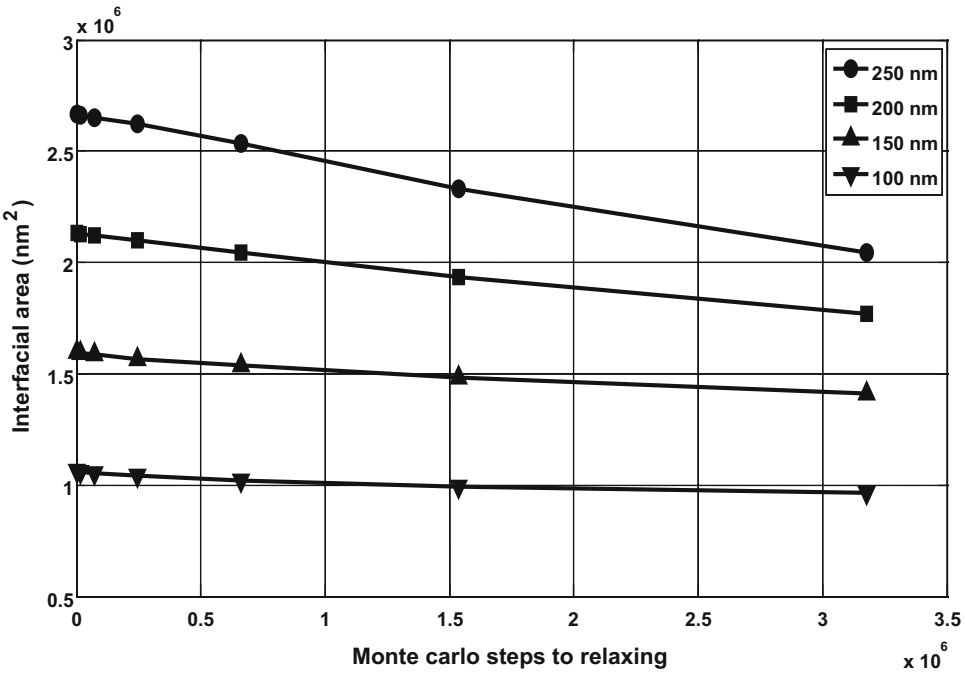

Fig. 2 Interfacial area (nm^2) as a function of Monte Carlo steps for different thickness of BHJ layer

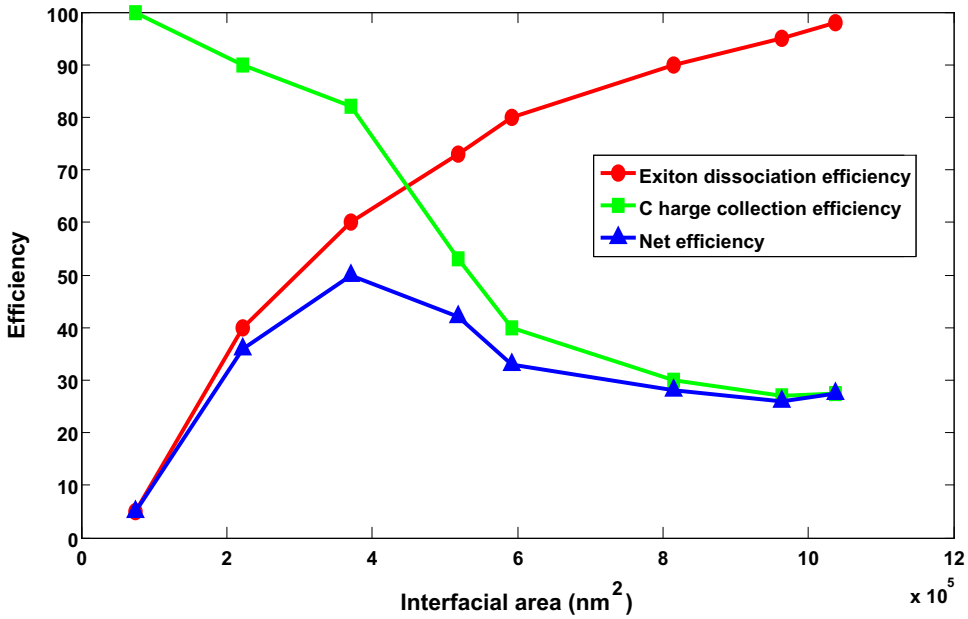

Fig. 3 Exciton dissociation efficiency as a function of interfacial area

Table 1 The simulation parameters for the relaxed morphologies

Parameter	Value
Lattice length	60 nm
Lattice width	60 nm
Lattice height	100–250 nm
Lattice spacing	1 nm
Exciton generation rate	10 nm^{-3} s^{-1} [18]
Energetic disorder	75 meV [18]
Exciton lifetime	500 ps [18]
Exciton dissociation rate constant	10^3 ps^{-1} [18]
Dielectric constant	3.5 [34]
Cutoff distance	15 nm [19]
Temperature	300 K

enhances charge collection efficiency [23]. Monte Carlo simulation of the transport in a disordered medium has shown that the charge carrier mobility is very sensitive to morphology. The charge carrier mobility for holes is also affected by the morphology of the film, since the relative orientation of the conjugated polymer chains determines the degree of interchain interactions. This has recently been evidenced by theoretical studies on interchain interactions in conjugated polymers [36].

On the other hand, the exciton dissociation increases by increase in the interfacial area, whereas the charge collection efficiency will decrease as the interfacial area increases. By balancing these two competitive component efficiencies, two optimal morphologies are obtained. However, with low interfacial area (Fig. 1b), the pure phases are not perfectly separated due to the Ising model, and thus, many small isolated islands remain in those majority phases. These islands can act as traps for the free charges that can only be gotten rid of by waiting for the opposite charges to recombine at the interface between the islands and the majority phases. Therefore, the charge collection efficiency for Fig. 1b cannot reach the 100 % level as expected, but a peak can occur at a large-scale phase separation.

The mobility is calculated from the average distance that the charge carriers have moved along the direction of the field (Eq. 10) and increases with a decrease in the energetic disorder. Therefore, diffusion coefficient along the direction of the field increases with a decrease in the energetic disorder [30].

D_J, as a function of the applied bias of working, is depicted in Fig. 5. It can be seen that the values of diffusion coefficient change at low voltages and exhibit a rather constant value that starts to slightly decrease for voltages approaching V_{oc}. A similar slight increment in D_J was identified using other polythiophene derivatives in an electrochemical transistor setup [16].

These films exhibit low charge carrier mobility because films are mostly amorphous or disordered with respect to dopant position and site energy. Various techniques such as annealing and irradiation are often employed to reduce the disorder so as to improve carrier mobility. These techniques essentially change the film morphology by creating more ordered regions in amorphous polymer films. In fact, ordered regions can reduce the overall energetic/positional disorder in the material and thus enhances the mobility, but substantially influences the charge transport mechanism [37]. It is found from Fig. 5 that the diffusion coefficient

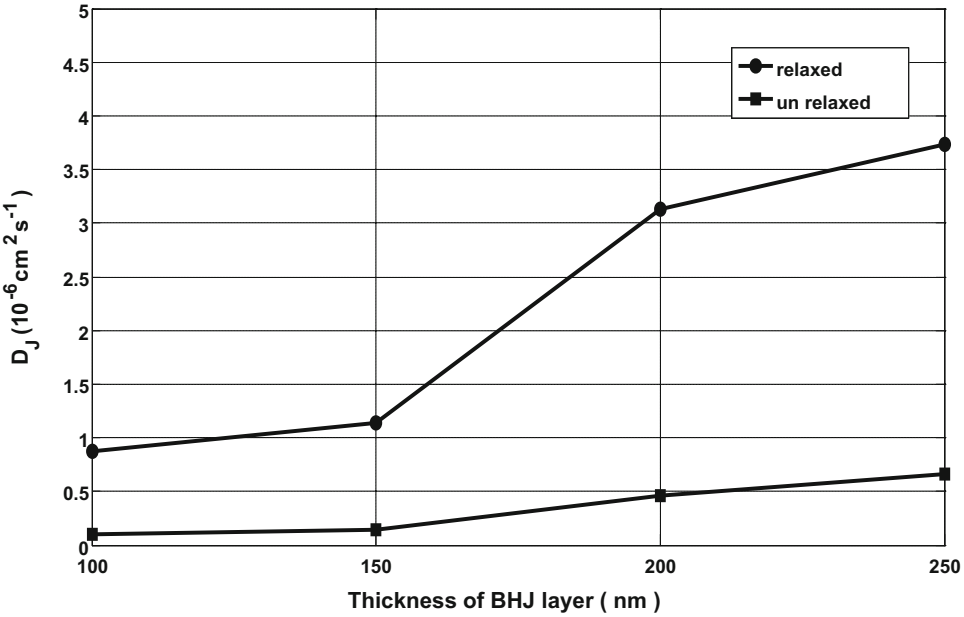

Fig. 4 Jump diffusion coefficients (D_J) as a function of thickness of BHJ layer at relaxed and unrelaxed (10^6 MC steps) systems

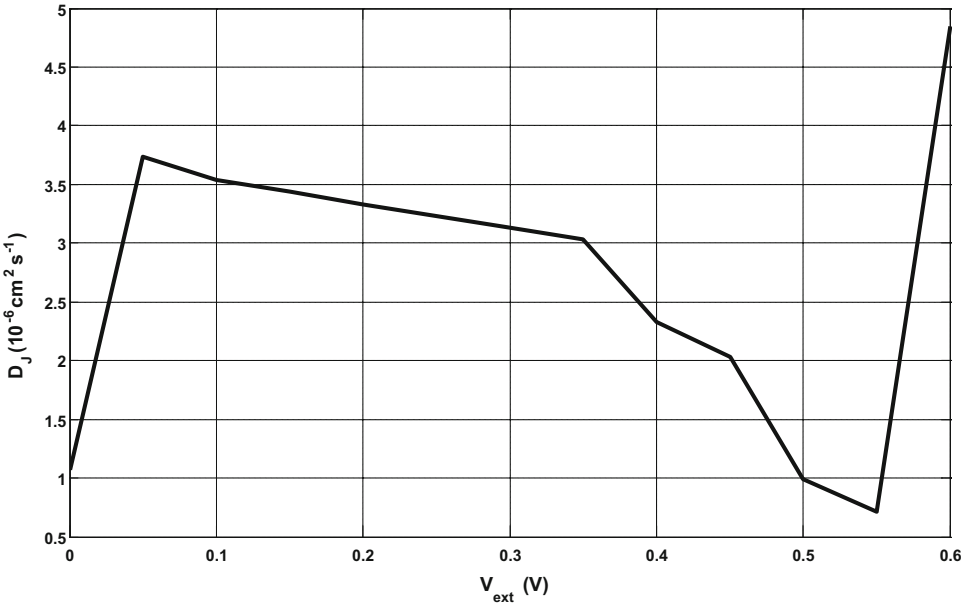

Fig. 5 Jump diffusion coefficient as a function of applied bias of working (*thickness* of active layer = 200 nm)

does not change noticeably with the applied voltage. When the voltage was changed from 0 to 0.6 V, the diffusion coefficient did not change remarkably with voltage variation. Because the direction of the hole flow was away from the electrode for $V > V_{OC}$, these carriers were instead captured by the electrode. In this case, the direction of the diffusion and the drift current was the same which resulted in increasing diffusion of carriers [38].

To determine the optimum PCBM:P3HT ratio, different ratios of the two materials were examined. Previous studies on the blend ratios randomly looked at a wide number of weight ratios such as 1:0.8–1:3 [39, 40]. Some other studies, however, have mentioned PCBM:P3HT = 1:1 as the optimal ratio [39], while others have mentioned 1:0.80 or 1:0.43 [41]. Results from these studies pointed out that the blend ratio 1:0.9 had high D_J values (Fig. 6). In the mentioned range of PCBM:P3HT ratio, the maximum power conversion efficiency has been reported for PCBM:P3HT of 1:0.9. A balanced diffusion of both electron and hole was obtained at the PCBM:P3HT = 1:0.9 ratio. Therefore, an enhancement of the charge carrier transport occurred by a larger mobility and a reduced recombination. In this blend ratio, both electron and hole transports were clearly non-dispersive.

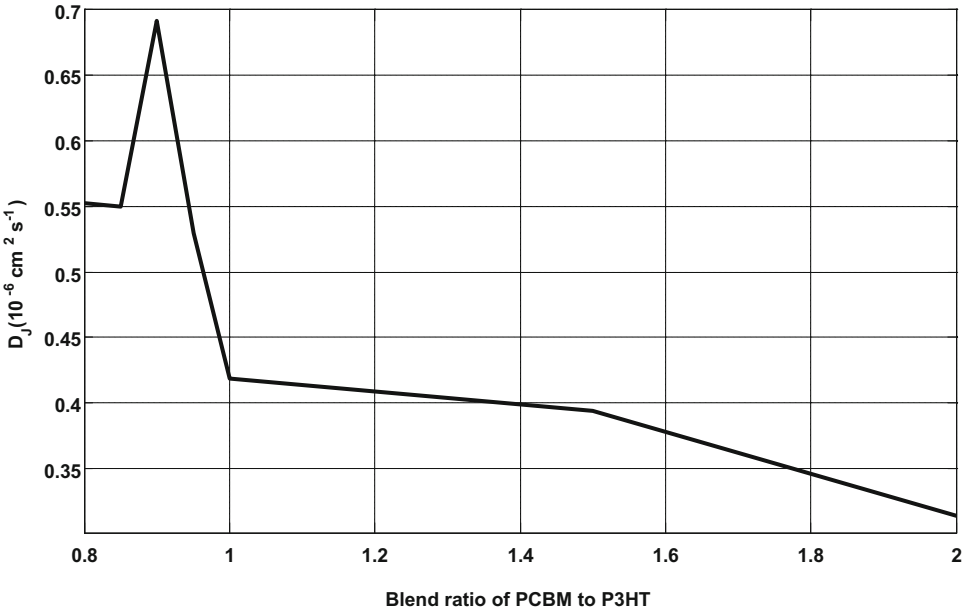

Fig. 6 Variation of diffusion coefficient as a function of PCBM:P3HT weight ratio

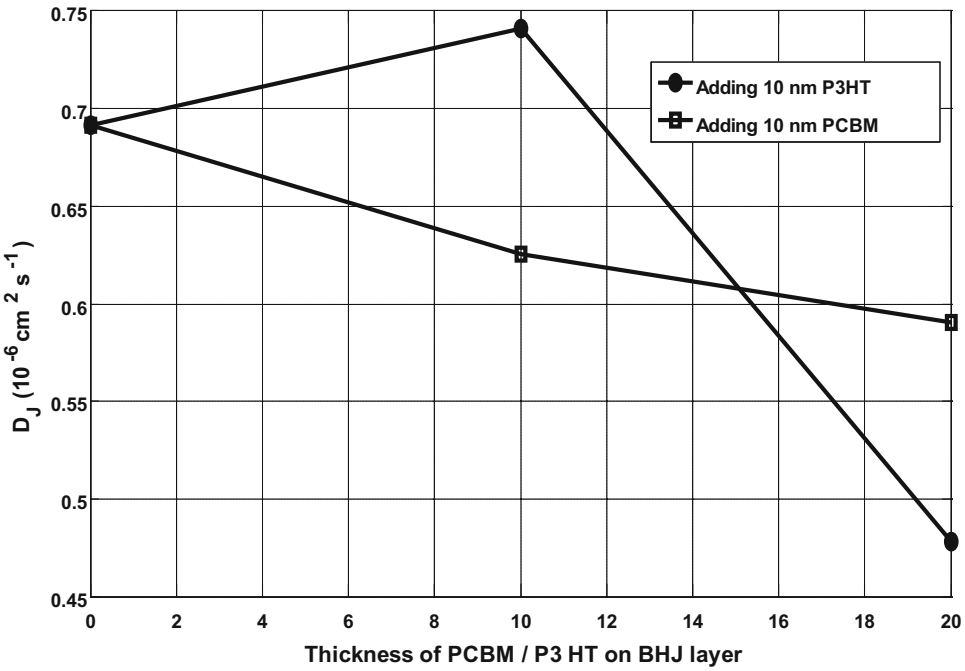

Fig. 7 Diffusion coefficient as a function of thickness of P3HT- or PCBM-coated BHJ layer (*thickness* of BHJ layer = 200 nm)

In Fig. 7, D_J increases with applied P3HT layer at the short-circuit condition in which the recombination occurs mostly near the semiconductor and electrode interface and there is no substantial recombination in the bulk. Applying a P3HT film of 10 nm thickness over the BHJ layer increases diffusion of electrons. In this case, the number of carriers increases. Adding P3HT films having more than 10 nm increases the carriers which reduce the mobility of carrier and the diffusion decreases. The recombination near the electrode can be regarded as dark carrier recombination.

Current density (J_{sc}) as a function of voltage is shown in Fig. 8. The results extracted from Fig. 8 (Table 2) show that short-circuit current (J_{sc}) and efficiency increased with adding a 10-nm P3HT layer, but open-circuit voltage (V_{oc}) and fill factor (FF) remained constant. At the short-circuit condition, the recombination occurs mostly near semiconductor and electrode interface and there is less recombination in the bulk. Adding a donor polymer at the anode side improves charge collection which decreases recombination near the electrode. In a photovoltaic device, the

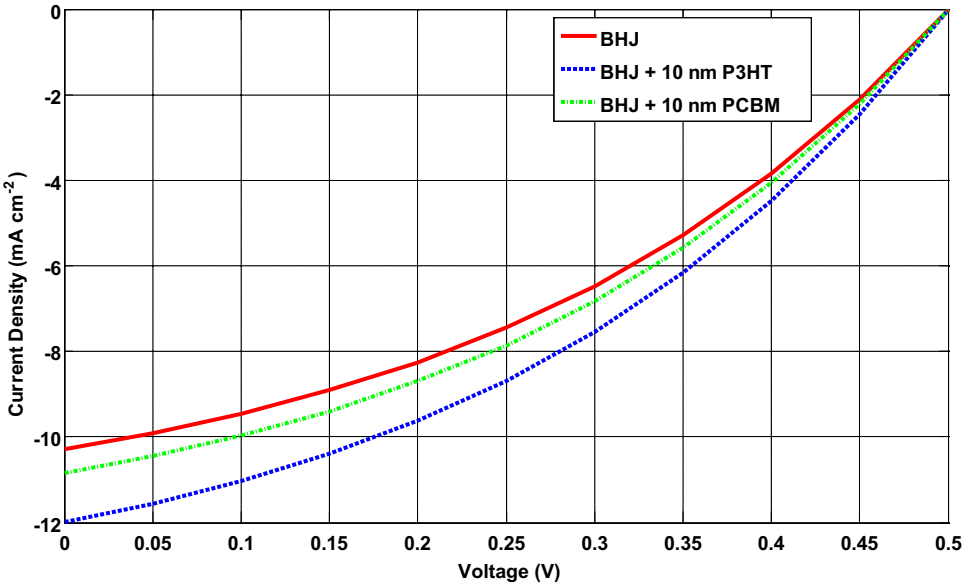

Fig. 8 Current density–voltage (J–V) characteristics of P3HT:PCBM BHJ solar cells

Table 2 The data extracted from Fig. 8

Sample	J_{SC} (mA/cm^2)	V_{OC} (V)	FF (%)	PCE (%)
Bulk	10.23	0.50	37.77	5.11
Bulk + 10 nm P3HT to anode side	11.12	0.50	37.77	5.56
Bulk + 10 nm PCBM to cathode side	10.84	0.50	37.77	5.42

short-circuit current is also due to light absorption; thus, the oscillatory nature of the short-circuit current is likely due to an optical effect. In this case, adding P3HT increases the production rate of exciton [4]. On the other hand, adding a PCBM layer at the cathode side was able to manipulate the energy-level alignment between photoactive layer and cathode to ensure an ohmic contact for electron transport and collection. Moreover, it should behave as an efficient hole blocking layer so that electrons were selectively extracted. Additionally, some cathode interfacial layer materials can be used as optical spacer to enhance photon absorption in high-efficiency PSCs, or to depress surface/interfacial recombination [42].

4 Conclusions

In this work, the effects of different parameters on the charge carrier mechanism and short-circuit current of P3HT:PCBM bulk heterojunction organic solar cell were investigated. It was shown that short-circuit current density and maximum power conversion efficiency occurred at 1:0.9 P3HT:PCBM weight ratio, while open-circuit voltage remained constant. It was also shown that the diffusion coefficient did not vary with applied bias of working. Adding a P3HT film with thickness of 10 nm over BHJ layer increased diffusion which decreased recombination and increased short-circuit current. Adding PCBM to cathode side increased short-circuit current by manipulate the energy-level alignment between photoactive layer and cathode to ensure an ohmic contact for electron transport and collection.

References

1. H.-E. Tseng, T.-H. Jen, K.-Y. Peng, S.-A. Chen, Measurements of charge mobility and diffusion coefficient of conjugated electroluminescent polymers by time-of-flight method. Appl. Phys. Lett. **84**, 1456–1458 (2004)
2. P. Morvillo, E. Bobeico, S. Esposito, R. Diana, Effect of the active layer thickness on the device performance of polymer solar cells having [60]PCBM and [70]PCBM as electron acceptor. Energy Procedia **31**, 69–73 (2012)
3. P. Vanlaekea, A. Swinnen, I. Haeldermansb, G. Vanhoyland, T. Aernoutsa, D. Cheyns, C. Deibel, J. D'Haen, P. Heremans, J. Poortmans, J.V. Manc, P3HT/PCBM bulk heterojunction solar cells: relation between morphology and electro-optical characteristics. Sol. Energy Mater. Sol. Cells **90**, 2150–2158 (2006)
4. D.W. Sievers, V. Shrotriya, Y. Yang, Modeling optical effects and thickness dependent current in polymer bulk-heterojunction solar cells. J. Appl. Phys. **100**, 114509 (2006)
5. M.M. Mandoc, L.J.A. Koster, P.W.M. Blom, Optimum charge carrier mobility in organic solar cells. Appl. Phys. Lett. **90**, 133504 (2007)

6. J. Jo, J.-R. Pouliot, D. Wynands, S.D. Collins, J.Y. Kim, T.L. Nguyen, H.Y. Woo, Y. Sun, M. Leclerc, A.J. Heeger, Enhanced efficiency of single and tandem organic solar cells incorporating a Diketopyrrolopyrrole-based low-band gap polymer by utilizing combined ZnO/Polyelectrolyte electron-transport layers. Adv. Mater. **25**, 4783–4788 (2013)
7. K. Vandewal, J. Widmer, T. Heumueller, C.J. Brabec, M.D. McGehee, K. Leo, M. Riede, A. Salleo, Increased open-circuit voltage of organic solar cells by reduced donor-acceptor interface area. Adv. Mater. **26**, 3839–3843 (2014)
8. L.H. Nguyen, H. Hoppe, T. Erb, S. Günes, G. Gobsch, N.S. Sariciftci, Effects of annealing on the nanomorphology and performance of poly(alkylthiophene):fullerene bulk-heterojunction solar cells. Adv. Funct. Mater. **17**, 1071–1078 (2007)
9. Y. Huang, E.J. Kramer, A.J. Heeger, G.C. Bazan, Bulk heterojunction solar cells: morphology and performance relationships. Chem. Rev. **114**, 7006–7043 (2014)
10. A. Ng, X. Liu, C.H. To, A.B. Djurišić, J.A. Zapien, W.K. Chan, Annealing of P3HT:PCBM blend film-the effect on its optical properties. ACS Appl. Mater. Interfaces **5**, 4247–4259 (2013)
11. Q. Wu, M. Bhattacharya, L.M.J. Moore, S.E. Morgan, Air processed P3HT:PCBM photovoltaic cells: morphology correlation to annealing, degradation, and recovery. J. Polym. Sci. Part B Polym. Phys. **52**, 1511–1520 (2014)
12. J.T. Shieh, C.H. Liu, H.F. Meng, S.R. Tseng, Y.C. Chao, S.F. Horng, The effect of carrier mobility in organic solar cells. J. Appl. Phys. **107**, 084503 (2010)
13. S. Günes, H. Neugebauer, N.S. Sariciftci, Conjugated polymer-based organic solar cells. Chem. Rev. **107**, 1324–1338 (2007)
14. J. Bisquert, Chemical diffusion coefficient of electrons in nanostructured semiconductor electrodes and dye-sensitized solar cells. J. Phys. Chem. B **108**, 2323–2332 (2004)
15. C. He, L. Zhao, Z. Zheng, F. Lu, Determination of electron diffusion coefficient and lifetime in dye-sensitized solar cells by electrochemical impedance spectroscopy at high Fermi level conditions. J. Phys. Chem. C **112**, 18730–18733 (2008)
16. T.R. Sanchis, A. Guerrero, J. Bisquert, G.G. Belmonte, Diffusion-recombination determines collected current and voltage in polymer:fullerene solar cells. J. Phys. Chem. C **116**, 16925–16933 (2012)
17. S.R. Mohan, M.P. Singh, M.P. Joshi, L.M. Kukreja, Monte Carlo simulation of carrier diffusion in organic thin films with morphological inhomogeneity. J. Phys. Chem. **117**, 24663–24672 (2013)
18. P.K. Watkins, A.B. Walker, G.L.B. Verschoor, Dynamical Monte Carlo modelling of organic solar cells: the dependence of internal quantum efficiency on morphology. Nano Lett. **5**, 1814–1818 (2005)
19. L. Meng, Y. Shang, Q. Li, Y. Li, X. Zhan, Z. Shuai, R.G.E. Kimber, A.B. Walker, Dynamic Monte Carlo simulation for highly efficient polymer blend photovoltaics. J. Phys. Chem. B **114**, 36–41 (2010)
20. G. Dennler, A.J. Mozer, G. Juska, A. Pivrikas, R. Osterbacka, A. Fuchsbauer, N.S. Sariciftci, Charge carrier mobility and lifetime versus composition of conjugated polymer/fullerene bulk-heterojunction solar cells. Org. Electron. **7**, 229–234 (2006)
21. A. Gadisa, *Studies of Charge Transport and Energy Level in Solar Cells Based on Polymer/Fullerene Bulk Heterojunction* (Ph.D. Thesis, Linköping University, Sweden, 2006)
22. J. Zhu, F. Liu, G.B. Stringfellow, S.H. Wei, Strain-enhanced doping in semiconductors: effects of dopant size and charge state. Phys. Rev. Lett. **105**, 195503 (2010)
23. J.H. Yap, T.T. To, S. Adams, Monte Carlo morphological modelling of a P3HT:PCBM bulk heterojunction organic solar cell. J. Polym. Sci. Part B Polym. Phys. **53**, 270–279 (2015)
24. N.W. Ashcroft, N.D. Mermin, *Solid State Physics* (Holt, Rinehart and Winston, New York, 1976)
25. N.E. Coates, I.-W. Hwang, J. Peet, G.C. Bazan, D. Moses, A.J. Heeger, 1,8 octanedithiol as a processing additive for bulk heterojunction materials: Enhanced photoconductive response. Appl. Phys. Lett. **93**, 072105 (2008)
26. W. Ming, Z.Z. Fang, F. Liu, Effects of Li doping on H-diffusion in MgH_2: a first-principles study. J. Appl. Phys. **114**, 243502 (2013)
27. M. Ansari-Rad, J.A. Anta, J. Bisquert, Interpretation of diffusion and recombination in nanostructured and energy-disordered materials by stochastic quasi equilibrium simulation. J. Phys. Chem. C **117**, 16275–16289 (2013)
28. M. Jakobsson, *Monte Carlo Studies of Charge Transport Below the Mobility Edge* (LiU-Tryck, Sweden, 2012)
29. A.B. Walker, A. Kambili, S.J. Martin, Electrical transport modelling in organic electroluminescent devices. J. Phys.: Condens. Matter **14**, 9825–9876 (2002)
30. F. Jansson, A.V. Nenashev, S.D. Baranovskii, F. Gebhard, R. Österbacka, Effect of electric field on diffusion in disordered materials. Ann. Phys. **18**, 856–862 (2009)
31. H. Bassler, Charge transport in disordered organic photoconductors. Phys. Status Solidi B **175**, 15–56 (1993)
32. M. C. Heiber, *Dynamic Monte Carlo Modeling of Exciton Dissociation and Geminate Recombination in Organic Solar Cells* (Ph.D. thesis, University of Akron, 2012)
33. S.R. Mohan, M.P. Joshi, M.P. Singh, Charge transport in disordered organic solids: a Monte Carlo simulation study on the effects of film morphology. Org. Electron. **9**, 355–368 (2008)
34. V. Paul Robbiano, *Simulations of Organic Solar Cells with an Event-Driven Monte Carlo Algorithm, Master of Science* (The Graduate Faculty of the University of Akron, Akron, 2011)
35. L. Oum, J.M.R. Parrondo, H.L. Martinez, Combined effect of periodic gates and external fields on the diffusion coefficient of a single particle. Phys. Rev. E **67**, 011106 (2003)
36. S.E. Shaheen, C.J. Brabec, N.S. Sariciftci, F. Padinger, T. Fromherz, J.C. Hummelen, 2.5 % Efficient organic plastic solar cells. Appl. Phys. Lett. **78**, 841–843 (2001)
37. S.R. Mohan, M.P. Joshi, M.P. Singh, Negative electric field dependence of mobility in TPD doped polystyrene. Chem. Phys. Lett. **470**, 279–284 (2009)
38. J.-K. Park, J.-C. Kang, S.Y. Kim, B.H. Son, J.Y. Park, S. Lee, Y.H. Ahn, Diffusion length in nanoporous photoelectrodes of dye-sensitized solar cells under operating conditions measured by photocurrent microscopy. J. Phys. Chem. Lett. **3**, 3632–3638 (2012)
39. G. Kalonga, G.K. Chinyama, M.O. Munyati, M. Maaza, Characterization and optimization of poly (3- hexylthiophene-2, 5-diyl) (P3HT) and [6, 6] phenyl-C61- butyric acid methyl ester (PCBM) blends for optical absorption. J. Chem. Eng. Mater. Sci. **4**, 93–102 (2013)
40. G. Dennler, M.C. Scharber, C.J. Brabec, Polymer-fullerene bulk-heterojunction solar cells. Adv. Mater. **21**, 1323–1338 (2009)
41. L. Salamandra, *Organic Photo-Voltaic Cells and Photo-Detectors based on Polymer Bulk-Heterojunctions* (Ph.D. Thesis, University of Rome, 2010)
42. B. Xiao, H. Wu, Y. Cao, Solution-processed cathode interfacial layer materials for high-efficiency polymer solar cells. Mater. Today **18**(7), 385–394 (2015)